9-27-2006

A Nd Isotopic Study of Southern Sourced Waters and Indonesian Throughflow at Intermediate Depths in the Cenozoic Indian Ocean

Ellen E. Martin
University of Florida, emartin@geology.ufl.edu

Howie Scher
University of South Carolina - Columbia, hscher@geol.sc.edu

Publication Info

Published in *Geochemistry, Geophysics, Geosystems*, Volume 7, Issue 9, 2006, pages 1-14.
Martin, E. E. & Scher, H. (2006). A Nd isotopic study of southern sourced waters andIndonesian Throughflow at intermediate depths in the Cenozoic Indian Ocean. *Geochemistry, Geophysics, Geosystems, 7* (9), 1-14.

Geochemistry Geophysics Geosystems G3
AN ELECTRONIC JOURNAL OF THE EARTH SCIENCES
Published by AGU and the Geochemical Society

Article
Volume 7, Number 9
27 September 2006
Q09N02, doi:10.1029/2006GC001302
ISSN: 1525-2027

A Nd isotopic study of southern sourced waters and Indonesian Throughflow at intermediate depths in the Cenozoic Indian Ocean

Ellen E. Martin

Department of Geological Sciences, University of Florida, 241 Williamson Hall, P.O. Box 112120, Gainesville, Florida 32611, USA (emartin@geology.ufl.edu)

Howie Scher

Department of Geological Sciences, University of Florida, 241 Williamson Hall, P.O. Box 112120, Gainesville, Florida 32611, USA

Now at Ocean Sciences Department, University of California, Santa Cruz, Santa Cruz, California 95064, USA (howie@ucsc.edu)

[1] We present Nd isotopic data for fossil fish teeth recovered from the past 40 m.y. at ODP Site 757, currently located at 1650 m water depth on the Ninetyeast Ridge in the Indian Ocean. Although Site 757 sits in a region strongly influenced by weathering inputs from the Himalayas and volcanic inputs from the Indonesian arc, the pattern of Nd isotopic variations does not appear to respond to these potential sources of Nd. Instead, secular variations correlate to changes in the composition of intermediate to deep water masses bathing the site and circulation patterns in the Indian Ocean. From ~40 to 10 Ma, ε_{Nd} values and the pattern of change at Site 757 closely match those of ODP Site 1090, a deep water site in the Atlantic sector of the Southern Ocean. Comparison to data from several Fe-Mn crusts in the Indian Ocean suggests that intermediate to deep water flow paths were similar to the modern distribution of Circumpolar Deep Water. At approximately 10 Ma, Nd isotopic values increase in a step function by 2 ε_{Nd} units, suggesting that plate motions had carried Site 757 into a region influenced by Indonesian Throughflow. Estimates of the vertical and horizontal position of this site at 10 Ma imply that Indonesian Throughflow extended as far south as ~20°S and to a depth of ~1500 m. From 10 to 0 Ma, Nd isotopic variations at Site 757 appear to record variations in Indonesian Throughflow. From 10 to 5.5 Ma, values at Site 757 overlap with those from crusts located in the southwest Pacific, indicating extensive flow through the Indonesian Seaway. From 5.5 to 3.4 Ma, ε_{Nd} values become less radiogenic at Site 757 and more radiogenic in the southwest Pacific, suggesting increasing closure of the seaway and concomitant rerouting of equatorial Pacific waters. Beginning at 3.4 Ma, ε_{Nd} values become more radiogenic again at Site 757, which may be attributed to enhanced opening of the seaway or to a change in the source of Throughflow waters from a southern to a northern Pacific region.

Components: 9319 words, 6 figures, 2 tables.

Keywords: Nd isotopes; Indonesian Throughflow; paleocirculation; Indian Ocean; Cenozoic; ODP Site 757.

Index Terms: 1040 Radiogenic isotope geochemistry; 4924 Geochemical tracers; 4962 Thermohaline.

Received 10 March 2006; **Revised** 25 May 2006; **Accepted** 18 July 2006; **Published** 27 September 2006.

Martin, E. E., and H. Scher (2006), A Nd isotopic study of southern sourced waters and Indonesian Throughflow at intermediate depths in the Cenozoic Indian Ocean, *Geochem. Geophys. Geosyst.*, *7*, Q09N02, doi:10.1029/2006GC001302.

Theme: Past Ocean Circulation

1. Introduction

[2] Nd isotopes preserved in marine sediments record information about past water mass circulation, as demonstrated by studies that track the variability of North Atlantic Deep Water input into the Southern Ocean [*Rutberg et al.*, 2000; *Frank et al.*, 2002; *Piotrowski et al.*, 2004, 2005]. The power of this isotopic system as a proxy for water mass can be attributed to (1) the ~500–1000 year residence time of Nd in seawater [*Elderfield and Greaves*, 1982; *Piepgras and Wasserburg*, 1985; *Jeandel et al.*, 1995; *Tachikawa et al.*, 1999, 2003], which is shorter than the 1500 year mixing time of the oceans [*Broecker and Peng*, 1982], and (2) the dominance of dissolved and particulate continental sources of Nd to seawater that are delivered through rivers and atmospheric deposition [*Goldstein and Jacobsen*, 1987; *Elderfield*, 1988; *Jeandel*, 1993; *Tachikawa et al.*, 1999].

[3] Because the residence time of Nd is so close to the mixing time of the oceans, Nd exhibits properties of both conservative and nonconservative water mass tracers; therefore it has been referred to as a "quasi-conservative" tracer [*Frank et al.*, 2002]. The extent to which this isotopic system can be applied to address critical questions concerning (1) paleoclimatology, such as the relationship between gateway events, thermohaline circulation and global climate change, versus (2) the intensity of continental weathering and resulting atmospheric CO_2 levels [e.g., *Ling et al.*, 1997; *O'Nions et al.*, 1998; *von Blanckenburg and Nagler*, 2001; *Frank*, 2002; *Piotrowski et al.*, 2005; *Scher and Martin*, 2004, 2006] depends on the extent of its conservative behavior.

[4] The nonconservative nature of Nd is documented by the increase in concentration along the thermohaline circulation flow path [*Jeandel et al.*, 1995, 1998; *Tachikawa et al.*, 1999, 2003; *Lacan and Jeandel*, 2001, 2005a, 2005b], as well as the process of "boundary exchange," in which Nd remobilized from lithogenic sources influences the isotopic composition, but not the Nd concentration, of water masses near the margins [*Tachikawa et al.*, 2004; *Lacan and Jeandel*, 2001, 2005a, 2005b]. In contrast, the correlation between Nd isotopes and other conservative properties, such as salinity, potential temperature [*Bertram and Elderfield*, 1993; *Jeandel et al.*, 1998] and silicate concentration [*Rutberg et al.*, 2000; *Goldstein and Hemming*, 2003] highlights the conservative nature of this isotopic system; as does the lack of a Himalayan Nd isotopic signature in the Indian Ocean [*Goldstein et al.*, 1984; *Albarède and Goldstein*, 1992; *Albarède et al.*, 1997; *O'Nions et al.*, 1998], despite the fact that Pb isotopes vary along mixing lines suggesting input from High Himalayan gneisses and leucogranites [*Frank and O'Nions*, 1998; *Vlastélic et al.*, 2001; *Frank*, 2002].

[5] Possible explanations posed for the conservative behavior of Nd isotopes in the Indian Ocean are that (1) Himalayan Nd is trapped in fan or estuarine sediments, (2) Himalayan Nd enters the surface ocean, but does not mix or sink, (3) additional radiogenic sources balance the Himalayan input, (4) the residence time of Nd is long enough to allow the signal to disperse more widely throughout the ocean, in which case it does not appear to substantially overprint the water mass signatures, or (5) the relative mass balance between Nd in the Himalayan source material and deep water minimizes the effect [*Albarède et al.*, 1997; *Frank and O'Nions*, 1998; *Frank*, 2002; *Frank et al.*, 2006]. Decoupling between Nd and Pb isotopes suggests that Pb enters the deep Indian Ocean through vertical cycling, while the Nd signature is largely carried in with deep water masses originating in the Southern Ocean. This supports the concept that Nd isotopic studies are useful for understanding circulation and that their application to studies of continental weathering may be limited to studies in specific source regions for water masses.

[6] Constraining the sources of non-conservative behavior of Nd isotopes is critical for the acceptance of this proxy. Therefore we developed a Nd isotopic record for Site 757, an intermediate depth site along the Ninetyeast Ridge, to determine whether a weathering signal from the Himalayas could be detected at a shallower depth. Our results suggest that the Nd isotopes for intermediate to deep water masses recorded at Site 757 are largely unaffected by weathering products from the Himalayas or the Indonesian Arc. Instead the isotopic

record from this site for the past 40 Ma appears to preserve a record of the source regions of water masses bathing the site, and therefore the circulation patterns through time. This basic pattern is modified by the lateral migration and vertical subsidence history of the Ninetyeast Ridge and by variations in the composition and magnitude of Indonesian Throughflow (ITF). As a result, the record also preserves a history of ITF for the past 10 m.y.

2. Background

2.1. Site Information

[7] ODP Site 757B is located at 17°01′S, 88°10′E near the crest of the Ninetyeast Ridge in 1650 m of water. Drilling at this site recovered ~220 m of sediment overlying ~155 m of ash and tuff, which in turn overlie basalt flows [*Peirce et al.*, 1989]. The pelagic sediment represents a relatively complete section from early Eocene through Pleistocene. This study focused on the section from 0–40 Ma, the interval represented by the rapid increase in $^{87}Sr/^{86}Sr$, which is generally attributed to input from the Himalayan uplift [*Hodell et al.*, 1989; *Edmond*, 1992; *Krishnaswami et al.*, 1992; *Palmer and Edmond*, 1992; *Richter et al.*, 1992]. The sediments for this interval are composed of a white to pale brown, bioturbated nannofossil ooze.

[8] Backtracking indicates that this site has been moving NNE with the Australian Plate. Estimates place it at approximately 30–35°S 40 Ma and ~20°S 20 Ma [*Zachos et al.*, 1992] (Figure 1). The subsidence history is a bit more confusing because there are two published estimates. On the basis of water depths indicated by benthic foraminifera, *Peirce et al.* [1989] determined that following aerial deposition of basalts in the late Paleocene the site subsided rapidly to 1500 m by the late Eocene with the final subsidence to 1650 m occurring after the middle Miocene. In contrast, *Zachos et al.* [1992] derived a more traditional subsidence curve using the equation $\Delta Z = kt^{1/2}$ [*Sclater et al.*, 1971] and an assumption of a depth of 0 m for the late Paleocene. For this interpretation water depths reached 1500 m approximately10 Ma.

2.2. Age Model

[9] The initial age model for Site 757 was based on nannofossil and planktonic foraminifera datums. This model was updated by *Zachos et al.* [2001] and *Billups and Schrag* [2003], who converted the datums to *Berggren et al.* [1995] and added constraints from $\delta^{18}O$ chemostratigraphy for the section from 30–52 Ma. This later model has been further revised for this study using Sr isotope chemostratigraphy (Table 1). An initial plot of the $^{87}Sr/^{86}Sr$ of foraminifera from Site 757 based on the age model from *Billups and Schrag* [2003] compared to the global seawater curve highlighted the presence of a condensed section or hiatus that was not defined by the biostratigraphic age model (Figure 2). This plot illustrates that there are errors in the published age models for the interval from 87–101 m. To correct for these errors without forcing each data point to fit on the seawater Sr curve, we generated a line through the data points representing 87–101 m (~16 to 24 Ma in Figure 2a) and a line through a linear segment of the seawater curve over the interval of interest, then migrated the data line onto the seawater line (Figure 2b). The result was the recognition of a condensed section or a hiatus between ~14.8 and 18.3 Ma. Additional sampling between 87 and 91 m would be required to precisely constrain the extent of missing or condensed section. The revised age model increases the age of the youngest samples in this section by 1.9 m.y. and the oldest samples by 4.1 m.y. This age model has been applied throughout this paper.

2.3. Modern Hydrology of the Region

[10] At 1650 m water depth, Site 757 is currently bathed in Indian Deep Water (IDW), a water mass characterized by potential temperatures between 1.25 and 4°C, a salinity maximum of ~34.7–34.8, and oxygen values ~4.7 ml/l [*Jeandel et al.*, 1998; *Tomczak and Godfrey*, 2003]. This water mass ranges from 500–3800 m in the southern portion of the Indian Ocean to 2000–3800 m in the north, with a core at approximately 2400 m. There is a gradual transition between the underlying Antarctic Bottom Water (AABW) and IDW, such that some authors refer to these water masses as upper and lower deep water. These two water masses flow northward together from their source in the Southern Ocean (Figure 1c). The physical properties of IDW suggest it originates as North Atlantic Deep Water (NADW) that is carried into the Indian Ocean with the Antarctic Circumpolar Water (CPW) [*Tomczak and Godfrey*, 2003].

[11] *Jeandel et al.* [1998] determined that the ε_{Nd} value of IDW is approximately −6.1 (where ε_{Nd} represents the deviation in parts per 10^4 of the $^{143}Nd/^{144}Nd$ ratio relative to the chondritic uniform reservoir [*DePaolo and Wasserburg*, 1976]). This is significantly more radiogenic than NADW or CPW,

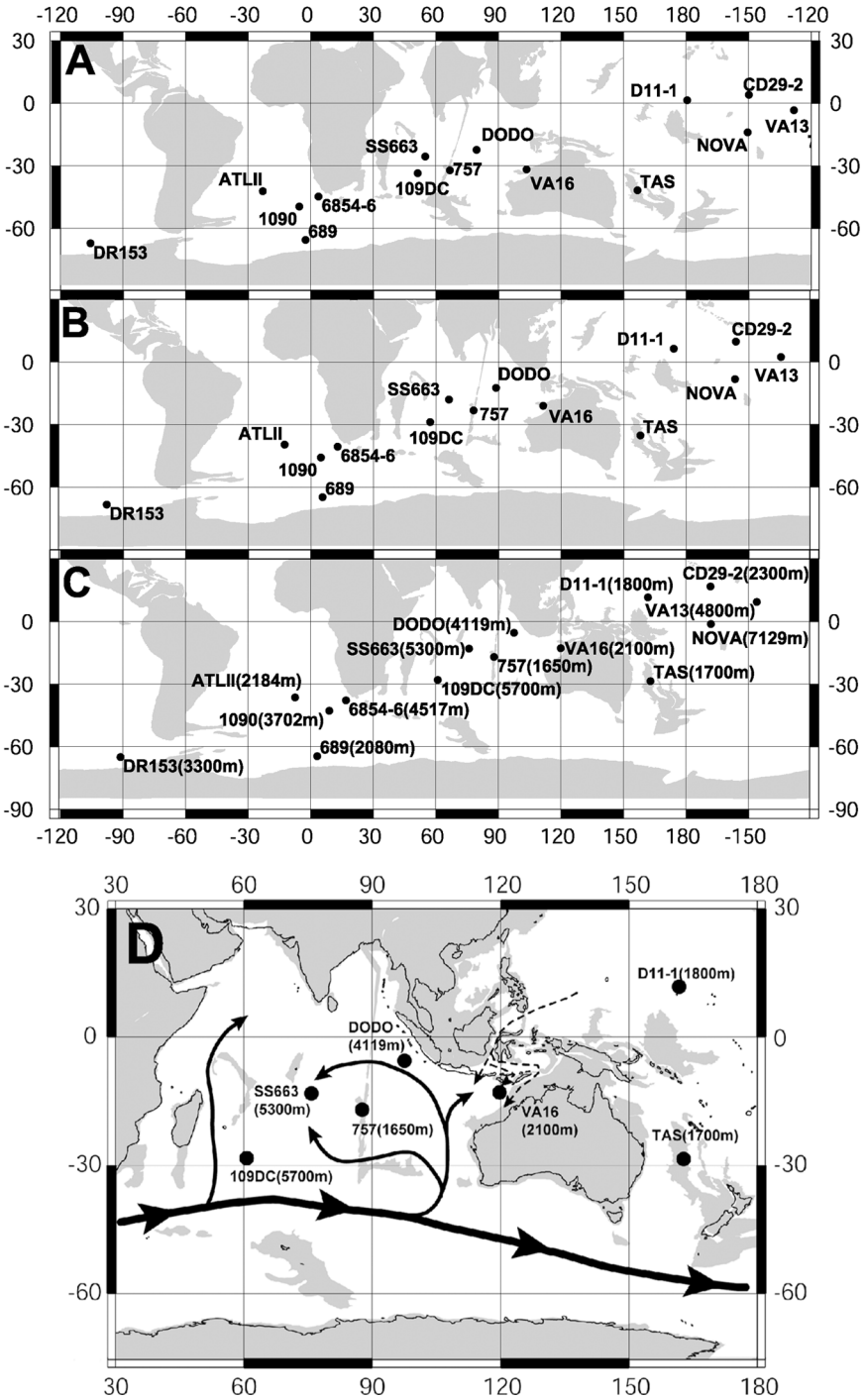

Figure 1. Reconstructions and location maps highlighting sites discussed in the text. (a) Reconstruction for 40 Ma. (b) Reconstruction for 20 Ma. (c) Modern locations with current water depths in meters listed in parentheses. (d) A modern map of the primary region of interest for this study. Solid lines illustrate deep water flow paths for the Indian Ocean based on *Mantyla and Reid* [1995] and *Frank et al.* [2006]. Dashed lines indicate the shallow pathway for Indonesian Throughflow based on *Gordon and Fine* [1996]. All four reconstructions were created using ODSN (http://www.odsn.de).

Table 1. Sr Isotopic Data for Foraminifera and Age Model for Site 757

Sample core-sec, cm	Depth, mbsf	Age,[a] Ma	Age,[b] Ma	$^{87}Sr/^{86}Sr$[c]	Error
2H-2, 42–50	6.46	1.04	1.04	0.709130	0.000013
2H-6, 75–83	12.78	2.09	2.09	0.709097	0.000010
3H-4, 125–131	19.78	3.32	3.32	0.709037	0.000013
4H-4, 114–120	29.27	4.32	4.32	0.709040	0.000014
4H-5, 40–47	30.03	4.40	4.40	0.709052	0.000013
5H-4, 124–130	38.97	5.34	5.34	0.709096	0.000014
5H-5, 80–87	40.04	5.45	5.45	0.709072	0.000011
5H-C, 5–9	41.52	5.61	5.61	0.708991	0.000013
6H-4, 110–116	48.43	6.34	6.34	0.708977	0.000018
6H-5, 113–120	49.96	6.50	6.50	0.708976	0.000014
7H-3, 58–65	56.11	7.48	7.48	0.708920	0.000011
7H-6, 24–32	60.28	8.02	8.02	0.708929	0.000016
8H-2, 130–137	65.03	8.65	8.65	0.708890	0.000013
9H-1, 10–19	71.95	9.56	9.56	0.708898	0.000011
9H-1, 13–20	71.96	9.56	9.56	0.708889	0.000010
9H-2, 82–88	74.15	10.25	10.25	0.708876	0.000014
9H-4, 10–18	76.44	11.07	11.07	0.708875	0.000011
9H-5, 82–88	78.65	11.86	11.86	0.708816	0.000013
10H-4, 1–3	86.02	14.50	14.50	0.708630	0.000011
10H-4, 83–91	86.87	14.80	14.80	0.708795	0.000010
10H-4, 95–102	87.01	14.85	14.85	0.708786	0.000011
11H-1, 0–6	91.22	16.36	18.29	0.708459	0.000011
11H-2, 130–136	94.03	17.36	19.93	0.708487	0.000028
11H-4, 33–41	96.07	18.09	21.15	0.708375	0.000014
11H-4, 35–43	96.08	18.10	21.16	0.708447	0.000014
11H-4, 136–144	97.10	18.46	21.77	0.708425	0.000011
11H-5, 122–130	98.46	18.95	22.58	0.708273	0.000013
11H-6, 45–53	99.19	19.21	23.05	0.708325	0.000011
11H-6, 106–114	99.81	19.43	23.38	0.708155	0.000014
11H-7, 18–26	100.42	19.65	23.75	0.708201	0.000014
12H-1, 30–35	101.13	23.96	23.96	0.708170	0.000014
12H-, 120–124	102.02	25.03	25.03	0.708159	0.000013
12H-2, 18–26	102.52	25.64	25.64	0.708146	0.000022
12H-4, 68–76	106.02	29.45	29.45	0.708047	0.000010
12H-5, 29–37	107.13	29.67	29.67	0.708073	0.000011
12H-6, 9–17	108.42	29.92	29.92	0.708167	0.000016
13H-1, 57–63	111.10	31.57	31.57	0.707933	0.000014
13H-5, 47–54	117.00	32.64	32.64	0.707862	0.000011
13H-6, 96–104	119.00	32.90	32.90	0.707791	0.000011
14H-2, 49–59	122.14	33.74	33.74	0.707749	0.000014
14H-4, 76–84	125.40	34.54	34.54	0.707792	0.000017
15H-1, 130–137	131.14	36.22	36.22	0.707726	0.000013
15H-2, 123–131	132.57	37.28	37.28	0.707735	0.000013
15H-5, 105–113	136.89	40.50	40.50	0.707654	0.000011
16H-2, 13–21	141.12	43.66	43.66	0.707664	0.000013

[a] Age model based on biostratigraphic ages [*Peirce et al.*, 1989] converted to *Berggren et al.* [1995] and modified by $\delta^{18}O$ chemostratigraphy by *Zachos et al.* [2001] and *Billups and Schrag* [2003].
[b] Age model modified to reflect Sr isotope chemostratigraphy (this paper).
[c] $^{87}Sr/^{86}Sr$ normalized to $^{86}Sr/^{88}Sr$ = 0.1194; NIST 987 = 0.710245 ±0.000024 (2σ) based on repeat analyses over several years; internal precision for all samples is usually less than the external precision.

which have values closer to −11 and −8 respectively in the South Atlantic [*Jeandel*, 1993]. On the basis of temperature, salinity and oxygen, IDW is believed to form by vertical mixing of waters sourced from the Southern Ocean and Indonesian Intermediate Water (IIW), the lower limb of ITF [*Fieux et al.*, 1996]. The Nd isotopes support this interpretation given that southern sourced deep water values are ∼−8 [*O'Nions et al.*, 1998] and IIW has a value ∼−4 [*Jeandel et al.*, 1998].

[12] ITF develops because sea level tends to be higher in the western Pacific than the eastern Indian Ocean. The resulting pressure gradient transports Pacific thermocline waters into the Indonesian archipelago, where they are mixed and modified before flowing into the Indian Ocean.

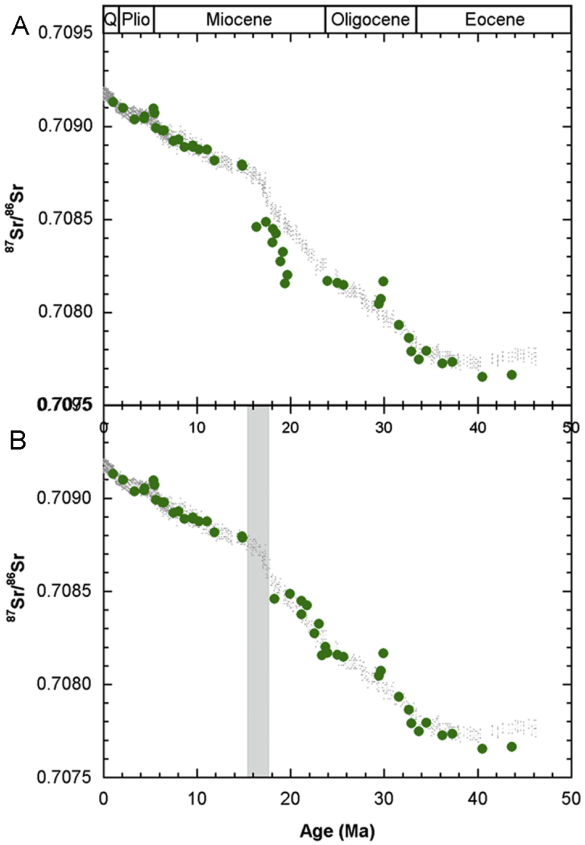

Figure 2. $^{87}Sr/^{86}Sr$ data for foraminifera (solid green circles) from Site 757. The gray dots represent the seawater curve including the analytical error of ±0.000023 for each data point, thereby forming an envelope of seawater values [*Hodell and Woodruff*, 1994; *Farrell et al.*, 1995; *Mead and Hodell*, 1995; *Martin et al.*, 1999]. The symbols for the foraminifera data are larger than the error bars. (a) Foraminifera $^{87}Sr/^{86}Sr$ values plotted using the original age model from *Peirce et al.* [1989] updated to the timescale by *Berggren et al.* [1995] and modified with oxygen isotope chemostratigraphy by *Zachos et al.* [2001] and *Billups and Schrag* [2003]. The foraminifera data plot below the seawater curve for the interval from 16 to 20 Ma. Outside of that interval the forams consistently plot on the seawater curve. This pattern suggests the presence of a hiatus or condensed section that was not identified by previous age models. (b) The revised age model for Site 757 based on Sr isotope chemostratigraphy for the interval originally from 16 to 20 Ma. For the revised age model a straight line was fit to the data from 16 to 20 Ma at Site 757 and migrated onto a straight-line segment of the seawater curve. The gray bar highlights the interval represented by a hiatus or condensed section.

The magnitude of this throughflow varies seasonally [*Gordon et al.*, 1997]. The Indonesian region consists of a series of poorly connected deep basins that are constantly evolving as the Australian plate drifts northward and the Indonesian Island Arc develops. Today ITF occurs as a jet of low salinity water (~34.55‰) centered between 10 and 14°S in the Indian Ocean and extending to ~1200 m [*Talley and Baringer*, 1997; *Gordon et al.*, 1997]. Most of the waters in the ITF are currently sourced from the relatively fresh, cool thermocline waters of the North Pacific that travel to the Indian Ocean by way of the Makassar Strait and Banda Sea [*Gordon and Fine*, 1996; *Fieux et al.*, 1996; *Gordon et al.*, 1997, 1999].

[13] Another water mass common at intermediate depths in the Indian Ocean is Antarctic Intermediate Water (AAIW), which forms a salinity minimum centered at 1000 m. This water mass can be traced up to ~10° to 18°S. Northward progress beyond that point is blocked by equatorial currents [*Talley and Baringer*, 1997; *Tomczak and Godfrey*, 2003]. There are no modern data on the Nd isotopic composition of AAIW in the Indian Ocean, but values from the Atlantic and Pacific range from −6.2 to −8.9 [*Jeandel*, 1993; *Lacan and Jeandel*, 2005a].

2.4. History of the Indonesian Throughflow

[14] The intensity and composition of ITF waters have varied through time. Prior to the Miocene, the Tethys seaway in this region was relatively open and a strong connection existed between the Pacific and Indian Ocean basins. The record of the closure of the Tethys in the Indonesian region is complex, but a combination of geotectonic, paleobiological, and isotopic data suggest that there was progressive restriction of the seaway from the early to the late Miocene. Geotectonic reconstructions indicate that interarc spreading in the middle Miocene permitted flow through this region, but these pathways became more limiting during the middle to late Miocene [*Linthout et al.*, 1997; *Nishimura and Suparka*, 1997] and were largely closed in the latest Miocene (~6 Ma [*Nishimura and Suparka*, 1997]). Following this interval of limited flow, *Nishimura and Suparka* [1997] argue that the combination of local tectonics and sea level variations renewed shallow flow paths through the Indonesian Seaway in the Pliocene.

[15] These tectonic interpretations are corroborated by the presence of distinct foraminiferal assemblages in the eastern and western Pacific during the early Miocene, reflecting flow through the Indonesian Seaway and the development of a gradient in the depth of the thermocline across the Pacific [*Kennett et al.*, 1985]. By the late Miocene, how-

ever, similar taxa are identified in the eastern and western Pacific, suggesting development of the Equatorial Undercurrent in response to restriction of the seaway. In addition, oxygen isotopic results support the development of a warm surface water pool in the western equatorial Pacific in the late Miocene [*Gasperi and Kennett*, 1993]. A comparison of foram assemblages between the equatorial Indian and Pacific Oceans also found that deep dwelling planktonic assemblages began to diverge in the latest Miocene, while shallow assemblages indicated continued shallow water connections [*Srinivasan and Sinha*, 1998]. Finally, a Nd isotopic study of an Fe-Mn crust from the Tasman Sea recorded increasing influence of Pacific waters starting around 10 Ma, reflecting closure of the Indonesian Seaway and redirection of deep Pacific currents to the south [*van de Flierdt et al.*, 2004].

[16] In addition to variations in the intensity of the flow, *Cane and Molnar* [2001] argue that a change in the source waters of the ITF occurred approximately 4 Ma. Prior to this time the ITF was dominated by a warmer, saltier source from the South Pacific. Following tectonic changes ~4 Ma the South Pacific flow was redirected to the south and replaced by the cooler, fresher thermocline waters from the North Pacific.

3. Methods

[17] Fish teeth and foraminifera were handpicked from the greater than 125 μm fraction of bulk ODP samples that were disaggregated by sonication in deionized water. The teeth were cleaned using the oxidative-reductive cleaning technique developed by Boyle [*Boyle*, 1981; *Boyle and Keigwin*, 1985; *Rosenthal et al.*, 1997]. Foraminifera were broken open and sonicated to remove material inside the chambers. Sr and REE were separated from the fish teeth by standard column chemistry techniques using Mitsubishi resin with HCl as an eluent. Nd and Sm were later separated on a second column using Mitsubishi resin and hydroxyisobuteric acid as the eluent. Blanks for these procedures are 100 pg Sr and 10 pg Nd. Sr was extracted from samples of foraminifera using Sr Spec resin and a technique modified from *Pin and Bassin* [1992]. Blanks for this procedure are 150 pg Sr.

[18] Isotopic ratios were analyzed on a Micromass Sector 54 thermal ionization mass spectrometer. Nd samples were loaded on zone refined Re filaments with silica gel and analyzed as NdO^+. A beam of 400–500 mV $^{142}Nd^{16}O$ was monitored for 200 ratios. The value for the Ames standard run with the samples was 0.512138 ± 0.000014 (2σ) (n = 40), and the value for JNdi was 0.512102 ± 0.000014 (2σ) (n = 120). A subset of four samples was spiked for Nd and Sm to determine the $^{147}Sm/^{144}Nd$ value, which averaged 0.1229. This is consistent with the ratio reported for fish teeth from other studies [*Thomas et al.*, 2003; *Scher and Martin*, 2004]. $^{87}Sr/^{86}Sr$ was analyzed by monitoring an ^{88}Sr beam of 1.5V for 200 ratios. The long-term average for NIST 987 over a period of several years is 0.710245 ± 0.000023 (2σ).

4. Results

[19] Site 757 was sampled at a relatively coarse resolution with an average of approximately one sample every 2.5 m.y. from 40–10 Ma, and one sample every 0.7 m.y. from 10 to 0 Ma. Because of this low resolution we plan to only discuss the general trends in the data, not the details of smaller variations. Data from this site (Table 2) are plotted in Figure 3. The general trends can be divided into three segments: (1) the section from 40 to 11 Ma, (2) a step function increase between 10.9 and 10.2 Ma, and (3) the final segment from 10.2 to 0.6 Ma. The first segment increases gradually from −7.5 $\varepsilon_{Nd(T)}$ units to a maximum of −6 at 31.5 Ma followed by a return to −7.5 by 11 Ma. Values jump by 2 $\varepsilon_{Nd(T)}$ units from −7.5 to −5.5 over the interval from 10.9 to 10.2 Ma. More data would be required to accurately define the rate and nature of this shift. In the final segment $\varepsilon_{Nd(T)}$ values average −5.2, but vary between −4.6 and −5.8 from 10.2 to 6.1 Ma. Values start to decrease at 6.1 Ma reaching a minimum of −6.6 at 3.4 Ma. The last three data points increase to −5.7, a value that is similar to modern IDW [*Jeandel et al.*, 1998; *Frank et al.*, 2006].

5. Discussion

5.1. 40 to 10 Ma

[20] The increasing $\varepsilon_{Nd(T)}$ trend from 40 and 31.5 Ma at Site 757 probably reflects the introduction of radiogenic input from the Pacific, but at this time the source region appears to be the Southern Ocean rather than the Tethys region. Although the Indonesian Seaway was relatively unrestricted at this time (Figure 1a), Site 757 was located between 35 and 30°S [*Zachos et al.*, 1992], placing it too far south for direct influence from ITF. In the Southern Ocean a similar pattern of increasing $\varepsilon_{Nd(T)}$ is

Table 2. Nd Isotopic Data for Site 757

Sample core-sec, cm	Depth, m	Age,[a] Ma	Age,[b] Ma	$^{143}Nd/^{144}Nd$[c]	2σ	$\varepsilon_{Nd(0)}$	$\varepsilon_{Nd(T)}$[d]	2σ	[Nd], ppm
1H-cc, 0–2	3.91	0.61	0.61	0.512339	±14	−5.83	−5.83	±0.28	252
2H-2, 42–50	6.46	1.04	1.04	0.512346	±12	−5.70	−5.68	±0.24	184
"	6.46	1.04	1.04	0.512346	±13	−5.70	−5.68	±0.26	184
2H-4, 100–107	10.03	1.63	1.63	0.512310	±16	−6.40	−6.38	±0.32	180
3H-5, 31–38	20.35	3.38	3.38	0.512296	±17	−6.68	−6.65	±0.34	233
5H-1, 88–95	34.12	4.83	4.83	0.512347	±10	−5.67	−5.63	±0.20	416
5H-cc, 0–17	40.10	5.74	5.74	0.512315	±17	−6.31	−6.25	±0.34	64
6H-3, 48–54	46.31	6.11	6.11	0.512377	±07	−5.10	−5.04	±0.14	173
6H-5, 107–113	49.90	6.49	6.49	0.512336	±11	−5.90	−5.84	±0.22	65
6H-cc, 4–12	52.50	7.00	7.00	0.512368	±08	−5.26	−5.20	±0.16	152
7H-3, 144–150	56.97	7.59	7.59	0.512396	±09	−4.71	−4.64	±0.18	91
7H-6, 18–25	60.21	8.01	8.01	0.512359	±11	−5.44	−5.37	±0.22	153
7H-cc, 7–16	62.20	8.28	8.28	0.512367	±15	−5.28	−5.20	±0.30	121
8H-cc, 0–17	71.80	9.54	9.54	0.512363	±30	−5.36	−5.27	±0.58	93
9H-2, 73–82	74.08	10.23	10.23	0.512355	±12	−5.52	−5.42	±0.24	196
9H-4, 10–18	76.04	10.93	10.93	0.512246	±15	−7.65	−7.54	±0.30	158
10H-4, 1–3	86.02	14.50	14.50	0.512275	±19	−7.08	−6.95	±0.38	253
"	86.02	14.50	14.50	0.512269	±12	−7.20	−7.07	±0.24	253
"	86.02	14.50	14.50	0.512263	±11	−7.32	−7.18	±0.22	253
11H-2, 130137	94.03	17.36	19.93	0.512254	±13	−7.49	−7.30	±0.26	391
11H-5, 80–88	98.04	18.80	22.34	0.512273	±14	−7.12	−6.92	±0.28	389
12H-1, 120–124	102.02	25.03	25.03	0.512292	±14	−6.75	−6.51	±0.28	499
12H-3, 144–150	105.27	28.96	28.96	0.512286	±12	−6.87	−6.59	±0.24	306
12H-5, 110–115	108.07	29.85	29.85	0.512317	±13	−6.26	−5.98	±0.26	201
12H-6, 139–147	109.73	30.73	30.73	0.512303	±13	−6.53	−6.26	±0.26	254
13H-1, 57–63	111.10	31.57	31.57	0.512319	±13	−6.22	−5.93	±0.26	218
13H-3, 60–62	114.10	32.27	32.27	0.512296	±16	−6.67	−6.37	±0.32	139
14H-4, 76–84	125.40	34.54	34.54	0.512269	±16	−7.20	−6.87	±0.32	124
15H-1, 130–137	131.14	36.22	36.22	0.512260	±14	−7.37	−7.04	±0.28	177
15H-5, 105–113	136.89	40.50	40.50	0.512233	±15	−7.90	−7.52	±0.3	235

[a] Initial biostratigraphic age for Site 757 [*Peirce et al.*, 1989] converted to *Berggren et al.* [1995] and updated by *Zachos et al.* [2001] and *Billups and Schrag* [2003].
[b] Age model modified using Sr isotope chemostratigraphy (this paper).
[c] $^{143}Nd/^{144}Nd$ normalized to $^{146}Nd/^{144}Nd = 0.7219$; JNdi standard = 0.512102 ± 0.000014 (2σ) (n = 120). The minimum error plotted in figures is 0.28 ε_{Nd} units, equivalent to the ± 0.000014 uncertainty for repeat analysis of the standard.
[d] $\varepsilon_{Nd(T)}$ values calculated using an $^{147}Sm/^{144}Nd$ value of 0.1229.

observed at both sites 689 and 1090 (Figure 4), suggesting intermediate waters at Site 757 were derived from this region and varied in response to changes in these source waters.

[21] *Scher and Martin* [2006] argue that increasing values at the Southern Ocean sites reflect progressive opening and deepening of Drake Passage starting at 41 Ma, or near the oldest data point for Site 757. In addition, the most radiogenic Nd isotopic values at Site 757 (32 to 29 Ma) coincide with a hiatus at Site 1090 (Figure 4) that has been interpreted to reflect changes in bottom current activity at Agulhas Ridge [*Wildeboer Schut et al.*, 2002], again, related to deepening of Drake Passage [*Livermore et al.*, 2005; *Eagles et al.*, 2006]. As this passage gradually opened an increasing volume of radiogenic Pacific water would have been introduced into the nascent Circumpolar Water (CPW).

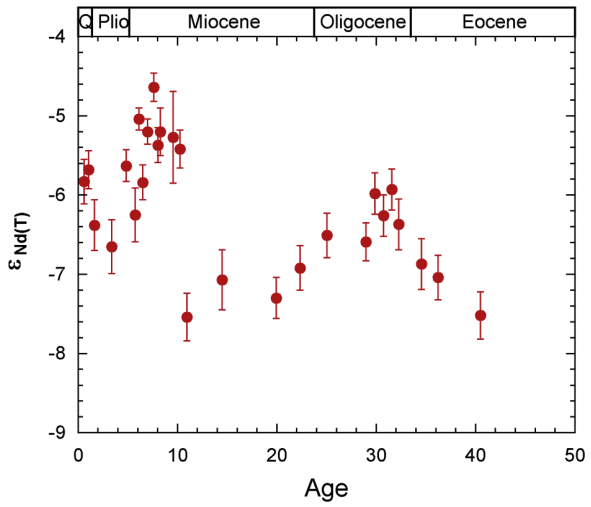

Figure 3. $\varepsilon_{Nd(T)}$ versus age for Site 757.

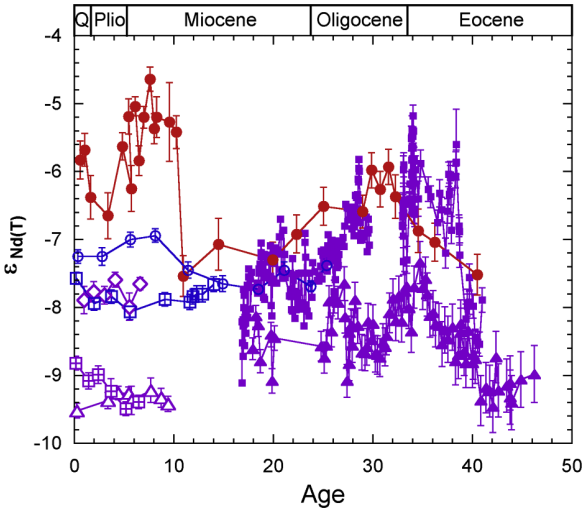

Figure 4. A comparison of Site 757 $\varepsilon_{Nd(T)}$ time series data (solid red circles) to published data from the Southern Ocean and deep Indian Ocean. Southern Ocean data are from fish teeth at Site 1090 (solid purple squares) [*Scher and Martin*, 2006] and Site 689 (solid purple triangles) [*Scher and Martin*, 2004], and from Fe-Mn crusts Atlantis II (open purple triangle), 6854-6 top (open purple squares with cross), and DR153 (open purple diamonds) [*Frank et al.*, 2002]. Deep Indian Ocean data are from Fe-Mn crusts SS-663 (open blue circles) and 109-DC (open blue squares) [*O'Nions et al.*, 1998]. Data from Site 757 track the deep Southern and Indian Ocean sites prior to the shift at 10.2 Ma. After the shift, there is little correlation between Site 757 and the other locations.

[22] Although the trends are similar at all three sites, the absolute $\varepsilon_{Nd(T)}$ values at Site 757 correlate most closely with the more radiogenic values at Site 1090 (Figure 4). It is surprising that the deeper site in the Southern Ocean records the greatest influence of Pacific waters; however, *Scher and Martin* [2006] suggest that the shallow Pacific waters entering through the passageway were entrained in deep water formation areas, while intermediate waters were ventilated in a region less influenced by the Pacific influx. The similarity between Sites 757 and 1090, therefore suggests that the intermediate waters in the Indian Ocean were derived from deep Southern Ocean waters similar to modern CPW.

[23] After 31.5 Ma Nd isotopic values at sites 1090 and 757 generally decrease. This trend may correspond to an increased influx of nonradiogenic deep waters from the North Atlantic, a predicted result of circumpolar circulation according to general ocean circulation models [*Mikolajewicz et al.*, 1993]. Alternatively the decreasing trend approaches $\varepsilon_{Nd(T)}$ values of −8 to −9, which would be consistent with enhanced production of Southern Ocean deep waters [*Piepgras and Wasserburg*, 1987; *Jeandel*, 1993; *Thomas et al.*, 2003; *Scher and Martin*, 2006]. The timing of the decreases at Sites 1090 and 757 coincides with the build up of ice on East Antarctica and cooling of high latitudes in the southern hemisphere [*Zachos et al.*, 2001], factors that are likely to contribute to greater production of Southern Ocean deep waters. Regardless of whether the decreasing pattern is generated by an increased flux of North Atlantic or Southern Ocean sourced waters, the shift to less radiogenic values appears to be a characteristic of CPW that is then transferred to the Indian Ocean site.

[24] The overlap in $\varepsilon_{Nd(T)}$ data between Fe-Mn crust SS663 in the Indian Ocean and Site 1090 from 24 to 18 Ma strengthens the argument for a circulation pattern similar to today's, whereby CPW flows into the deep Indian Ocean ultimate reaching SS663 in the Central Indian basin through a gap in the Ninetyeast Ridge [*Mantyla and Reid*, 1995]. Today waters at progressively shallower depths in the Indian Ocean record a greater influence from shallower Indian Ocean water masses and inputs from the Pacific; thus IDW is more radiogenic than the end-member CPW. In a similar fashion, Nd isotopes at Site 757 follow the trends at Sites 1090 and SS663, but are generally slightly more radiogenic (Figure 4).

[25] A comparison between Nd isotopic data from Site 757 and sites in the Pacific Ocean from 40 and 10 Ma [*Ling et al.*, 1997; *van de Flierdt et al.*, 2004] illustrates little similarity between records (Figure 5), supporting the idea that the Pacific influence in the Indian Ocean is derived from CPW, rather than ITF at this time. One exception is the "Nova" crust in the equatorial Pacific, which tracks Site 757 from 30 to 20 Ma. Variations at Nova have also been attributed to increased import of Southern Ocean waters via the CPW [*van de Flierdt et al.*, 2004]. The minor variations in Nd isotopes documented for crusts from the rest of the Pacific [*Ling et al.*, 1997; *van de Flierdt et al.*, 2004] and from the North Atlantic [*Burton et al.*, 1997, 1999] are distinct from the variations at Site 757 for this interval, adding to the argument that the variations seen in the Southern Ocean and Site 757 reflect changes in the percentage of Pacific, North Atlantic or Southern sourced deep waters at these locations, rather than changes in end-member compositions.

[26] An additional point about the Site 757 record over this interval is that it is not consistent with a pattern of influence from Himalayan runoff or

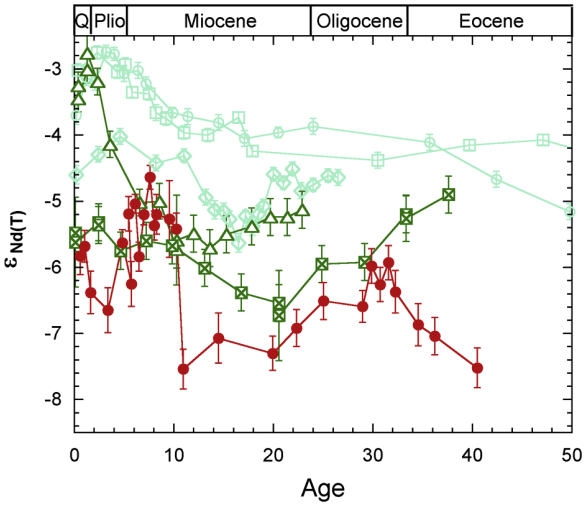

Figure 5. A comparison of Site 757 $\varepsilon_{Nd(T)}$ time series data (solid red circles) to published data from the Pacific Ocean. Pacific data from Fe-Mn crusts D11-1 (open green squares), CD29-2 (open green circles), and VA13 (open green diamonds) [*Ling et al.*, 1997], Tasman (open green triangle) and Nova (open green square with cross) [*van de Flierdt et al.*, 2004]. There is good agreement between Site 757, Tasman, and Nova from approximately 10 to 5 Ma; after that point, Tasman begins to increase while Site 757 decreases.

sediment remobilization from the Indonesian Arc. Variations in the isotopic compositions of (1) Sr, which has a residence time much longer than Nd, and (2) Pb, which has a residence time shorter than Nd, are believed to record Himalayan runoff and weathering of Indonesian arc material [*Hodell et al.*, 1989; *Edmond*, 1992; *Krishnaswami et al.*, 1992; *Palmer and Edmond*, 1992; *Richter et al.*, 1992; *Frank and O'Nions*, 1998; *O'Nions et al.*, 1998; *Frank et al.*, 2006], yet the pattern of change observed at Site 757 bears no resemblance to the seawater Sr isotope curve or the Pb isotope curves for Fe-Mn crusts in the Indian Ocean [*Frank et al.*, 2006].

5.2. Shift From 10.9 to 10.2 Ma

[27] Between 10.9 and 10.2 Ma $\varepsilon_{Nd(T)}$ values preserved at Site 757 shift dramatically by 2 ε_{Nd} units (Figure 5). The value after the shift is equivalent within error to the ~ -5.5 value recorded by south Pacific Fe-Mn crusts Nova and Tasman at this time [*van de Flierdt et al.*, 2004]. This convergence to Pacific $\varepsilon_{Nd(T)}$ values suggests that the backtracked location of 20°S for Site 757 was far enough north to be influenced by ITF and that the ITF was strong enough to affect the water column to a depth of 1500 m, the projected depth for Site 757 [*Peirce et al.*, 1989; *Zachos et al.*, 1992]. It also suggests that either the Pacific waters were relatively unmodified by weathering contributions during their journey through the Indonesian Seaway, or the final mixture of Southern Ocean sourced waters, Pacific waters, and arc weathering inputs coincidentally produced a value very similar to the Pacific end-member. The interpretation that the shift at Site 757 represents a transition from Southern Ocean sourced waters to waters sourced from the equatorial Pacific via ITF implies that there should be an associated shift in temperature. Surprisingly such a shift is not observed in Mg/Ca data from this site [*Billups and Schrag*, 2003].

5.3. 10.2 to 0.6 Ma

[28] Samples from 10.2 to 0.6 at Site 757 have $\varepsilon_{Nd(T)}$ values similar to modern IDW. This implies that throughout the record intermediate Indian Ocean waters represent Southern Ocean waters that are modified to varying degrees by ITF. The lack of an obvious relationship between the trend or the absolute values of the isotopic record at Site 757 and published records from the Southern Ocean after the shift at 10.9 Ma (Figure 4) underscores the idea that Site 757 had migrated into a region dominated by ITF.

[29] For approximately 5 m.y. following the shift, the $\varepsilon_{Nd(T)}$ values of ~ -5 to -5.5 recorded at Site

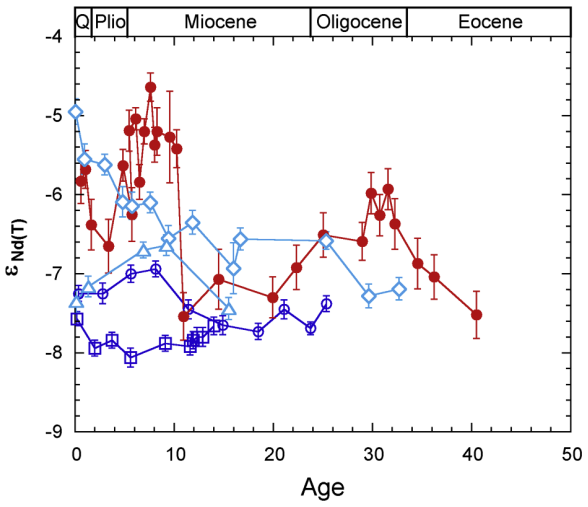

Figure 6. A comparison of Site 757 $\varepsilon_{Nd(T)}$ time series data (solid red circles) to published data from the Indian Ocean. Indian Ocean data from Fe-Mn crusts SS-663 (open blue circles) and 109-DC (open blue squares) [*O'Nions et al.*, 1998] and VA16 (open blue diamonds) and DODO (open blue triangles) [*Frank et al.*, 2006]. Values for Site 757 are distinct from other Indian Ocean sites after the shift around 10 Ma, reflecting the location and depth of each site relative to CPW and ITF.

757, Tasman and Nova [*van de Flierdt et al.*, 2004] are more radiogenic than values recorded at any other Indian Ocean site (Figures 5 and 6). For comparison, all other values within the Indian Ocean are <−6.6 (Figure 6), which may reflect depth variations between the sites. There is a general progression of increasingly radiogenic values within the Indian Ocean with distance along the flow path of deep and intermediate source waters from the Southern Ocean [*Mantyla and Reid*, 1995; *Vlastélic et al.*, 2001; *Frank et al.*, 2006] and with shallower depths. Site 757 is probably the only site shallow enough to be located in the main ITF. In contrast, DODO is ∼2500 m deeper and records a strong influence of CPW, similar to SS663. VA16 is ∼500 m deeper and appears to be largely influenced by Southern Ocean water or deeper outflow from the Indonesian Seaway at this time [*Frank et al.*, 2006], despite the fact that it is located closer to the seaway (Figure 1). In addition to depth considerations, the location of the greatest throughflow evolved with the tectonics of the region. During this interval the outflow may have been concentrated in a more westerly location and largely bypassed VA16.

[30] Beginning at ∼5.5 Ma the profiles for Site 757 and the Tasman crust start to diverge with $\varepsilon_{Nd(T)}$ values at Site 757 decreasing while those at Tasman increase rapidly (Figure 5). Both records can be interpreted in terms of progressive closure of the Indonesian Seaway and redirection of the Pacific waters that once flowed through the seaway toward south Pacific locations, such as Tasman Rise [*van de Flierdt et al.*, 2004]. This timing is consistent with closure estimates based on tectonic reconstructions and foraminiferal assemblage and isotopic data. Values at VA16 also start to increase at this time (Figure 6), suggesting a possible redirection of the outflow in the Indian Ocean as the seaway became more restricted. *Frank et al.* [2006] attribute the increase at VA16 to a stronger influence from arc weathering and boundary exchange; however, the signal of ITF waters at Site 757 does not record the same effect.

[31] The final trend observed at Site 757 is an increase starting 3.4 Ma that ends with IDW-type values [*Jeandel et al.*, 1998] for the past ∼1 m.y. This increase may represent renewed ITF at this time, consistent with tectonic interpretations of opening of the Sunda and Makassar Straits [*Nishimura and Suparka*, 1997]. Alternatively, the increase could reflect a change in the composition of the waters flowing through the seaway. As in the Indian Ocean, $\varepsilon_{Nd(T)}$ values in the Pacific tend in become more radiogenic with distance from the Southern Ocean and in shallower water [*Staudigel et al.*, 1985; *Piepgras and Jacobsen*, 1988] (Figure 5). This implies that waters sourced from the North Pacific are likely to be more radiogenic than those sourced from the South Pacific. The timing of the final increase at Site 757 coincides with a proposed switch from Southern to Northern Pacific source waters flowing through the Indonesian Seaway. Prior to 3 to 4 Ma the waters entering the seaway were warmer, saltier waters derived from the South Pacific. Around 3 to 4 Ma the Indonesian Archipelago, particularly in the region of Halmahera, evolved to the extent that it blocked the southern pathway and the current configuration was established with colder, fresher waters entering the seaway from the North Pacific [*Cane and Molnar*, 2001; *Gordon and Fine*, 1996]. Modern isotopic measurements from the thermocline depths that source the ITF in the Pacific are rare, but data from *Piepgras and Wasserburg* [1982] and *Piepgras and Jacobsen* [1988] suggest that a difference of ∼1 ε_{Nd} unit between the North and South Pacific is realistic.

6. Conclusions

[32] Secular variations in Nd isotopes preserved in fossil fish teeth at Site 757 on the Ninetyeast Ridge record the subsidence and backtracking history of this site, as well as variations in Southern Ocean and ITF source waters. From 40 to 10 Ma the waters at this site were dominated by intermediate to deep waters derived from the Southern Ocean. Although a true Antarctic Circumpolar Current did not exist throughout this entire interval, variations observed at Site 757 closely mimic those from the Cape Basin in terms of both the absolute value and the pattern of change. This implies that intermediate and deep waters were flowing from the Atlantic sector of the Southern Ocean into the Indian sector and then into the Indian Ocean, much as they do today. The correlation with deep rather than intermediate depth sites from the Atlantic sector of the Southern Ocean implies that the intermediate Indian Ocean waters were derived from a deep water mass similar to the modern CPW. A lack of correlation with the seawater Sr curve or Pb isotope records of Himalayan and Indonesian Arc influences in the Indian Ocean supports the idea that Nd isotopes in this basin did not respond to weathering inputs from the Himalayas or boundary exchange with volcanic material from the Indonesian region.

[33] Between 10.9 and 10.2 Ma Site 757 migrated far enough north to lie within the path of ITF. On the basis of backtracking estimates, this suggests that ITF extended as far south as ~20° and to a depth of ~1500 m at this time. From 10.2 Ma on the history of this site reflects the history of the ITF. The correlation between $\varepsilon_{Nd(T)}$ values at Site 757 and the Tasman crust indicates that the ITF was dominated by water from the South Pacific region and that the ITF composition was not significantly altered either during its transit through the Indonesian Seaway or by mixing in the Indian Ocean. The difference between Site 757 and crust VA16 during this interval also suggests a more northern flow path through the seaway than is observed today. The magnitude of the outflow, and therefore the extent of mixing with Indian Ocean waters, appears to be relatively constant until 5.5 Ma when it started to decrease, suggesting progressive closure of the Indonesian gateway. An increase in $\varepsilon_{Nd(T)}$ values starting at 3.5 Ma is consistent with either enhanced flow through the seaway, associated with the tectonic evolution of the region or a transition from ITF waters derived from the South Pacific to waters derived from the North Pacific.

Acknowledgments

[34] We would like to thank Alisa Haase for her contributions to this paper through her master's research. Ray Thomas, as always, kept the TIMS up and running. Comments by Martin Frank and an anonymous reviewer greatly improved the manuscript. Acknowledgment is made to the Donors of the American Chemical Society Petroleum Research Fund for partial support of this work. Additional support was provided by a National Science Foundation (NSF) grant to E.E.M. (OCE-9629370). The Ocean Drilling Program (OPD) provided samples; ODP is funded by the NSF under management of Joint Oceanographic Institutions (JOI).

References

Albarède, F., and S. L. Goldstein (1992), A world map of Nd isotopes in seafloor ferromanganese deposits, *Geology*, *20*, 761–763.

Albarède, F., S. L. Goldstein, and D. Dautel (1997), $^{143}Nd/^{144}Nd$ of Mn nodules from the Southern and Indian oceans, the global oceanic Nd budget, and their bearing on the deep ocean circulation during the Quarternary, *Geochim. Cosmochim. Acta*, *61*, 1277–1291.

Berggren, W. A., D. V. Kent, C. C. Swisher III, and M. P. Aubry (1995), A revised Cenozoic geochronology and chronostratigraphy, in *Geochronology, Time Scales and Global Stratigraphic Correlation*, edited by W. A. Berggren et al., *SEPM Spec. Publ.*, *54*, 129–212.

Bertram, C. J., and H. Elderfield (1993), The geochemical balance of the rare earth elements and neodymium isotopes in the oceans, *Geochim. Cosmochim. Acta*, *57*, 1957–1986.

Billups, K., and D. P. Schrag (2003), Application of benthic foraminiferal Mg/Ca ratios to questions of Cenozoic climate change, *Earth Planet. Sci. Lett.*, *209*, 181–195.

Boyle, E. A. (1981), Cadmium, zinc, copper and barium in foraminifera tests, *Earth Planet. Sci. Lett.*, *53*, 11–35.

Boyle, E. A., and L. D. Keigwin (1985), Comparison of Atlantic and Pacific paleochemical records for the past 215,000 y: Changes in deep ocean circulation and chemical inventories, *Earth Planet. Sci. Lett.*, *76*, 135–150.

Broecker, W. S., and T.-H. Peng (1982), *Tracers in the Sea*, 690 pp. Lamont-Doherty Geol. Observ., Palisades, N. Y.

Burton, K. W., H.-F. Ling, and R. K. O'Nions (1997), Closure of the Central American Isthmus and its effect on deep-water formation in the north Atlantic, *Nature*, *386*, 382–385.

Burton, K. W., D.-C. Lee, J. N. Christensen, A. N. Halliday, and J. R. Hein (1999), Actual timing of neodymium isotopic variations recorded by Fe-Mn crusts in the western North Atlantic, *Earth Planet. Sci. Lett.*, *171*(1), 149–156.

Cane, M. A., and P. Molnar (2001), Closing of the Indonesian seaway as a precursor to east African aridification around 3–4 million years ago, *Nature*, *411*, 157–162.

DePaolo, D. J., and G. J. Wasserburg (1976), Nd isotopic variations and petrogenetic models, *Geophys. Res. Lett.*, *3*, 249–252.

Eagles, G., R. Livermore, and P. Morris (2006), Small basins in the Scotia Sea: The Eocene Drake Passage gateway, *Earth Planet. Sci. Lett.*, *242*, 343–353.

Edmond, J. M. (1992), Himalayan tectonics, weathering processes, and the strontium isotope record in marine limestones, *Science*, *258*, 1594–1597.

Elderfield, H. (1988), The oceanic chemistry of the rare-earth elements, *Philos. Trans. R. Soc. London, Ser. A*, *325*, 105–126.

Elderfield, H., and M. J. Greaves (1982), The rare earth elements in seawater, *Nature*, *296*, 214–219.

Farrell, J. W., S. C. Clemens, and L. P. Gromet (1995), Improved chronostratigraphic reference curve of late Neogene seawater $^{87}Sr/^{86}Sr$, *Geology*, *23*, 403–406.

Fieux, M., R. Molcard, and A. G. Ilahude (1996), Geostrophic transport of the Pacific-Indian Oceans throughflow, *J. Geophys. Res.*, *101*, 12,421–12,432.

Frank, M. (2002), Radiogenic isotopes: Tracers of past ocean circulation and erosional input, *Rev. Geophys.*, *40*(1), 1001, doi:10.1029/2000RG000094.

Frank, M., and R. K. O'Nions (1998), Sources of Pb for the Indian Ocean ferromanganese crusts: A record of Himalayan erosion?, *Earth Planet. Sci. Lett.*, *158*, 121–130.

Frank, M., N. Whiteley, S. Kasten, J. R. Hein, and K. O'Nions (2002), North Atlantic Deep Water export to the Southern Ocean over the past 14 Myr: Evidence from Nd and Pb isotopes in ferromanganese crusts, *Paleoceanography*, *17*(2), 1022, doi:10.1029/2000PA000606.

Frank, M., N. Whiteley, T. van de Flierdt, B. C. Reynolds, and R. K. O'Nions (2006), Nd and Pb isotope evolution of deep water masses in the eastern Indian Ocean during the past 33 Myr, *Chem. Geol.*, *226*, 264–279.

Gasperi, J. T., and J. P. Kennett (1993), Vertical thermal structure evolution of Miocene surface waters: Western Equatorial Pacific DSDP Site 289, *Mar. Micropaleontol.*, *22*, 235–254.

Goldstein, S. L., and S. H. Hemming (2003), Long lived isotopic tracers in oceanography, paleoceanography, and ice sheet dynamics, in *Treatise on Geochemistry*, edited by H. Elderfield, pp. 453–489, Elsevier, New York.

Goldstein, S. L., and S. B. Jacobsen (1987), The Nd and Sr isotopic systematics of river-water dissolved material: Impli-

cations for the sources of Nd and Sr in the seawater, *Chem. Geol.*, *66*, 245–272.

Goldstein, S. L., R. K. O'Nions, and P. J. Hamilton (1984), A Sm-Nd isotopic study of atmospheric dusts and particulates from major river systems, *Earth Planet. Sci. Lett.*, *70*, 221–236.

Gordon, A. L., and R. Fine (1996), Pathways of water between the Pacific and Indian oceans in the Indonesian seas, *Nature*, *379*, 146–149.

Gordon, A. L., S. Ma, D. B. Olson, P. Hacker, A. Ffield, L. D. Talley, D. Wilson, and M. O. Baringer (1997), Advection and diffusion of Indonesian Throughflow with the Indian Ocean Southern Equatorial Current, *Geophys. Res. Lett.*, *24*, 2573–2576.

Gordon, A. L., R. D. Susanto, and A. Ffield (1999), Throughflow within Makassar Strait, *Geophys. Res. Lett.*, *26*, 3325–3328.

Hodell, D. A., and F. Woodruff (1994), Variations in the strontium isotopic ratio of seawater during the Miocene: Stratigraphic and geochemical implications, *Paleoceanography*, *9*, 405–426.

Hodell, D. A., P. A. Mueller, J. A. McKenzie, and G. A. Mead (1989), Strontium isotope stratigraphy and geochemistry of the Late Neogene, *Earth Planet. Sci. Lett.*, *92*, 165–178.

Jeandel, C. (1993), Concentration and isotopic compositions of Nd in the South Atlantic Ocean, *Earth Planet. Sci. Lett.*, *117*, 581–591.

Jeandel, C., J. K. Bishop, and A. Zindler (1995), Exchange of neodymium and its isotopes between seawater and small and large particles in the Sargasso Sea, *Geochim. Cosmochim. Acta*, *59*, 535–547.

Jeandel, C., D. Thouron, and M. Fieux (1998), Concentrations and isotopic compositions of neodymium in the eastern Indian Ocean and Indonesian straits, *Geochim. Cosmochim. Acta*, *62*, 2597–2607.

Kennett, J. P., G. Keller, and M. S. Srinivasan (1985), Miocene planktonic foraminiferal biogeography and paleoceanographic development of the Indo-Pacific, in *The Miocene Ocean: Paleoceanography and Biogeography*, edited by J. P. Kennett, *Mem. Geol. Soc. Am.*, *163*, 197–236.

Krishnaswami, S., J. R. Trivedi, M. M. Sarin, R. Ramesh, and K. K. Sharma (1992), Strontium isotopes and rubidium in the Ganges-Bramaputra river system: Weathering in the Himalaya, fluxes to the Bay of Bengal and contributions to the evolution of oceanic $^{87}Sr/^{86}Sr$, *Earth Planet. Sci. Lett.*, *109*, 243–253.

Lacan, F., and C. Jeandel (2001), Tracing Papua New Guinea imprint on the central Equatorial Pacific Ocean using neodymium isotopic compositions and rare earth element patterns, *Earth Planet. Sci. Lett.*, *186*, 497–512.

Lacan, F., and C. Jeandel (2005a), Acquisition of the neodymium isotopic composition of the North Atlantic Deep Water, *Geochem. Geophys. Geosyst.*, *6*, Q12008, doi:10.1029/2005GC000956.

Lacan, F., and C. Jeandel (2005b), Neodymium isotopes as a new tool for quantifying exchange fluxes at the continent-ocean interface, *Earth Planet. Sci. Lett.*, *232*, 245–257.

Ling, H. F., K. W. Burton, R. K. O'Nions, B. S. Kamber, F. von Blanckenburg, A. J. Gibb, and J. R. Hein (1997), Evolution of Nd and Pb isotopes in Central Pacific seawater from ferromanganese crusts, *Earth Planet. Sci. Lett.*, *146*, 1–12.

Linthout, K., H. Helmers, and J. Sopaheluwakan (1997), Late Miocene obduction and microplate migration around the southern Banda Sea and the closure of the Indonesian Seaway, *Tectonophysics*, *281*, 17–30.

Livermore, R., A. Nankivell, G. Eagles, and P. Morris (2005), Paleogene opening of Drake Passage, *Earth Planet. Sci. Lett.*, *236*, 459–470.

Mantyla, A. W., and J. L. Reid (1995), On the origins of deep and bottom waters of the Indian Ocean, *J. Geophys. Res.*, *100*, 2417–2439.

Martin, E. E., N. J. Shackleton, J. C. Zachos, and B. P. Flower (1999), Orbitally-tuned Sr isotope chemostratigraphy for the late middle to late Miocene, *Paleoceangraphy*, *14*, 74–83.

Mead, G. A., and D. A. Hodell (1995), Controls on the $^{87}Sr/^{86}Sr$ composition of seawater from the Middle Eocene to Oligocene: Hole 689B, Maud Rise, Antarctica, *Paleoceanography*, *10*, 327–346.

Mikolajewicz, U., E. Maier-Reimer, T. J. Crowley, and K.-Y. Kim (1993), Effect of Drake and Panamanian Gateways on the circulation of an ocean model, *Paleoceanography*, *8*, 409–426.

Nishimura, S., and S. Suparka (1997), Tectonic approach to the Neogene evolution of Pacific-Indian Ocean seaways, *Tectonophysics*, *281*, 1–16.

O'Nions, R. K., M. Frank, F. von Blanckenburg, and H. F. Ling (1998), Secular variation of Nd and Pb isotopes in ferromanganese crusts from the Atlantic, Indian and Pacific oceans, *Earth Planet. Sci. Lett.*, *155*(1–2), 15–28.

Palmer, M. R., and J. M. Edmond (1992), Controls over the strontium isotopic composition of river water, *Geochim. Cosmochim. Acta*, *56*, 2099–2111.

Peirce, J. W., et al. (1989), Site 757, *Proc. Ocean Drill. Program Initial Rep.*, *121*, 305–358.

Piepgras, D. J., and S. B. Jacobsen (1988), The isotopic composition of neodymium in the North Pacific, *Geochim. Cosmochim. Acta*, *52*, 1373–1381.

Piepgras, D. J., and G. J. Wasserburg (1982), Isotopic composition of neodymium in waters from the Drake Passage, *Science*, *217*, 207–214.

Piepgras, D. J., and G. J. Wasserburg (1985), Strontium and neodymium isotopes in hot springs on the East Pacific Rise and Guaymas Basin, *Earth Planet. Sci. Lett.*, *72*, 341–356.

Piepgras, D. J., and G. J. Wasserburg (1987), Rare earth element transport in the western North Atlantic inferred from Nd isotopic observations, *Geochim. Cosmochim. Acta*, *51*, 1257–1271.

Pin, C., and C. Bassin (1992), Evaluation of a Sr-specific extraction chromatographic method for isotopic analysis in geologic materials, *Anal. Chim. Acta*, *269*, 249–255.

Piotrowski, A. M., S. L. Goldstein, S. H. Hemming, and R. G. Fairbanks (2004), Intensification and variability of ocean thermohaline circulation through the last glaciation, *Earth Planet. Sci. Lett.*, *225*, 205–220.

Piotrowski, A. M., S. L. Goldstein, S. H. Hemming, and R. G. Fairbanks (2005), Temporal relationships of carbon cycling and ocean circulation at glacial boundaries, *Science*, *307*, 1933–1938, doi:10.1126/science.1104883.

Richter, F. M., D. B. Rowley, and D. J. DePaolo (1992), Sr isotope evolution of seawater: The role of tectonics, *Earth Planet. Sci. Lett.*, *109*, 11–23.

Rosenthal, Y., E. A. Boyle, and L. Labeyrie (1997), Last glacial maximum paleochemistry and deepwater circulation in the Southern Ocean: Evidence from foraminiferal cadmium, *Paleoceanography*, *12*, 787–796.

Rutberg, R. L., S. H. Hemming, and S. L. Goldstein (2000), Reduced North Atlantic Deep Water flux to the glacial Southern Ocean inferred from neodymium isotope ratios, *Nature*, *405*, 935–938.

Scher, H. D., and E. E. Martin (2004), Circulation in the Southern Ocean during the Paleogene inferred from Nd isotopes, *Earth Planet. Sci. Lett.*, *228*, 391–405.

Scher, H. D., and E. E. Martin (2006), Timing and consequences of the opening of Drake Passage, *Science*, *312*, 428–430, doi:10.1126/science.1120044.

Sclater, J. G., R. N. Anderson, and M. L. Bell (1971), The elevation of ridges and the evolution of the central Pacific, *J. Geophys. Res.*, *76*, 7888–7915.

Srinivasan, M. S., and D. K. Sinha (1998), Early Pliocene closing of the Indonesian Seaway: Evidence from north-east Indian Ocean and tropical Pacific deep-sea cores, *J. Asian Earth Sci. Lett.*, *16*, 29–44.

Staudigel, H., P. Doyle, and A. Zindler (1985), Sr and Nd isotope systematics in fish teeth, *Earth Planet. Sci. Lett.*, *76*, 45–56.

Tachikawa, K., C. Jeandel, and M. Roy-Barman (1999), A new approach to the Nd residence time in the ocean, *Earth Planet. Sci. Lett.*, *170*, 433–446.

Tachikawa, K., V. Athias, and C. Jeandel (2003), Neodymium budget in the modern ocean and paleo-oceanographic implications, *J. Geophys. Res.*, *108*(C8), 3254, doi:10.1029/1999JC000285.

Tachikawa, K., M. Roy-Barman, A. Michard, D. Thouron, D. Yeghicheyan, and C. Jeandel (2004), Neodymium isotopes in the Mediterranean Sea: Comparison between seawater and sediment signals, *Geochim. Cosmochim. Acta*, *68*, 3095–3106.

Talley, L. D., and M. O. Baringer (1997), Preliminary results from WOCE hydrographic sections at 80E and 32S in the central Indian Ocean, *Geophys. Res. Lett.*, *24*, 2789–2792.

Thomas, D. J., T. J. Bralower, and C. E. Jones (2003), Neodymium isotopic reconstructions of the late Paleocene-early Eocene thermohaline circulation, *Earth Planet. Sci. Lett.*, *209*, 309–322.

Tomczak, M., and J. S. Godfrey (2003), *Regional Oceanography: An Introduction*, 2nd ed., 390 pp., Daya, New Delhi.

van de Flierdt, T., M. Frank, A. N. Halliday, J. R. Hein, B. Hattendorf, D. Günther, and P. W. Kubik (2004), Deep and bottom water export from the Southern Ocean to the Pacific over the past 38 million years, *Paleoceanography*, *19*, PA1020, doi:10.1029/2003PA000923.

Vlastélic, I., W. Abouchami, S. J. G. Galer, and A. W. Hofmann (2001), Geographic control on Pb isotope distribution and sources in Indian Ocean Fe-Mn deposits, *Geochim. Cosmochim. Acta*, *65*, 4303–4319.

von Blanckenburg, F., and T. F. Nagler (2001), Weathering versus circulation-controlled changes in radiogenic isotope tracer composition of the Labrador Sea and North Atlantic Deep Water, *Paleoceanography*, *16*, 424–434.

Wildeboer Schut, E., G. Uenzelmann-Neben, and R. Gersonde (2002), Seismic evidence for bottom current activity at the Agulhas Ridge, *Global Planet. Change*, *34*, 185–198.

Zachos, J. C., D. K. Rea, K. Setp, R. Nomura, and N. Niitsuma (1992), Paleogene and Early Neogene deep water paleoceanography of the Indian Ocean as determined from benthic foraminifer stable carbon and oxygen isotope records, in *Synthesis of Results From Scientific Drilling in the Indian Ocean*, *Geophys. Monogr. Ser.*, vol. 70, edited by R. A. Duncan et al., pp. 351–385, AGU, Washington, D. C.

Zachos, J. C., M. Pagani, L. C. Sloan, E. Thomas, and K. Billups (2001), Trends, rhythms and aberrations in global climate 65 Ma to present, *Science*, *292*, 686–693.